

Toxic Synergism Between Quinolinic Acid and Glutaric Acid in Neuronal Cells Is Mediated by Oxidative Stress: Insights to a New Toxic Model

Paula Pierozan¹ · Ana Laura Colín-González^{1,2} · Helena Biasibetti¹ · Janaina Camacho da Silva¹ · Angela Wyse¹ · Moacir Wajner^{1,2,3} · Abel Santamaria² 

Received: 7 June 2017 / Accepted: 31 August 2017 / Published online: 21 September 2017
© Springer Science+Business Media, LLC 2017

Abstract It has been shown that synergistic toxic effects of quinolinic acid (QUIN) and glutaric acid (GA), both in isolated nerve endings and in vivo conditions, suggest the contribution of these metabolites to neurodegeneration. However, this synergism still requires a detailed characterization of the mechanisms involved in cell damage during its occurrence. In this study, the effects of subtoxic concentrations of QUIN and/or GA were tested in neuronal cultures, co-cultures (neuronal cells + astrocytes), and mixed cultures (neuronal cells + astrocytes + microglia) from rat cortex and striatum. The exposure of different cortical and striatal cell cultures to QUIN + GA resulted in cell death and stimulated different markers of oxidative stress, including reactive oxygen species (ROS) formation; changes in the activity of antioxidant enzymes such as superoxide dismutase, catalase, and glutathione peroxidase; and depletion of endogenous antioxidants such as -SH groups

and glutathione. The co-incubation of neuronal cultures with QUIN + GA plus the *N*-methyl-D-aspartate antagonist MK-801 prevented cell death but not ROS formation, whereas the antioxidant melatonin reduced both parameters. Our results demonstrated that QUIN and GA can create synergistic scenarios, inducing toxic effects on some parameters of cell viability via the stimulation of oxidative damage. Therefore, it is likely that oxidative stress may play a major causative role in the synergistic actions exerted by QUIN + GA in a variety of cell culture conditions involving the interaction of different neural types.

Keywords Quinolinic acid · Glutaric acid · Glutaric acidemia type I · Toxic synergism · Cell damage · Oxidative stress · Reactive gliosis

Paula Pierozan and Ana Laura Colín-González contributed equally to this work.

Electronic supplementary material The online version of this article (<https://doi.org/10.1007/s12035-017-0761-6>) contains supplementary material, which is available to authorized users.

✉ Moacir Wajner
mwajner@ufrgs.br

✉ Abel Santamaria
absada@yahoo.com

¹ Departamento de Bioquímica, Instituto de Ciências Básicas da Saúde, Universidade Federal do Rio Grande do Sul, Porto Alegre, RS, Brazil

² Laboratorio de Aminoácidos Excitadores, Instituto Nacional de Neurología y Neurocirugía Manuel Velasco Suárez, SSA, Insurgentes Sur 3877, 14269 Mexico City, Mexico

³ Serviço de Genética Médica, Hospital de Clínicas de Porto Alegre, Porto Alegre, RS, Brazil

Introduction

The metabolic recessive disease glutaric acidemia type I (GA I) is caused by deficiency of the activity of glutaryl-CoA dehydrogenase (GCDH, EC 1.3.99.7), an enzyme that participates in the catabolism of lysine, hydroxylysine, and tryptophan. The lack of activity of this enzyme induces the accumulation of high amounts of glutaric (GA) and 3-hydroxyglutaric (3-HGA) acids in different tissues, as well as in the blood, urine, and cerebrospinal fluid of patients with this disorder [1, 2]. Neurological symptoms are predominant in this cerebral organic acidemia. Macrocephaly and frontotemporal cortical atrophy are features observed at birth. Acute bilateral striatal degeneration occurs between 3 to 36 months of age following encephalopathic episodes often linked to infections, fever, or prolonged fasting; during these events, the concentrations of the accumulating metabolites reach millimolar

concentrations [3]. Then, patients progress toward dyskinesia, dystonia, hypotonia, seizures, muscle stiffness, and spasticity [2, 4–6].

Neurodegenerative disorders course with different toxic events, one of which is inflammation, a process that contributes to progression of cell and tissue damage. Several parameters of brain energy metabolism are affected by inflammatory processes, further accounting for oxidative stress and excitotoxicity [7–9]. Although release of inflammatory cytokines by microglia and macrophages in the CNS is associated with the pathogenesis of neurodegenerative disorders, the precise role of these molecules remains unsolved [10]. One of their known actions is the activation of the kynurenine pathway (KP), the catabolic pathway of tryptophan degradation, that results in the production of intermediate metabolites with neuroactive and/or redox properties. One of these metabolites, quinolinic acid (2,3-pyridine-dicarboxylic acid or QUIN), is necessary to adequate brain functioning when synthesized at normal levels [11, 12]; however, when produced in excess, it plays a toxic role, participating in neurological disorders coursing with excitotoxicity, such as Parkinson's and Huntington's diseases, as well as in GA I [12–14]. Despite QUIN has been shown to be able of inducing neurotoxic effects by different mechanisms [15], the most important is related with overactivation of *N*-methyl-D-aspartate receptors (NMDAr) and the subsequent increase of cytosolic Ca^{2+} concentration, further leading to free radical formation and oxidative damage, mitochondrial dysfunction, cytochrome c release, and ATP exhaustion [15, 16].

Regarding to GA I, several *in vitro* and *in vivo* studies have shown that both GA and 3-HGA, the most densely accumulated metabolites in this disorder, are also able to induce excitotoxicity, oxidative stress, and impairment of cellular energy metabolism in the rat brain [17–39]. Although this topic has already been extensively investigated, the toxic mechanisms underlying the acute striatal degeneration observed in GA I patients during metabolic decompensation are not yet well described. It has been suggested that QUIN, a metabolite that is increased during these processes, might potentially contribute to the striatal GA I pathogenesis, promoting severe neurological symptoms [14]. Noteworthy, it is known that the symptomatology of patients suffering from GA I worsens during infection or immunization. Therefore, the hypothesis that high accumulation of organic acids (GA and 3-HGA) during crises associated with increased concentrations of QUIN is potentially relevant to explain the pathophysiology of striatal damage in GA I patients. In turn, this concept suggests that these molecules could exert a toxic synergism to favor a scenario of neuronal cell dysfunction and brain tissue degeneration. In support to this concept,

we have recently demonstrated that QUIN can exert such synergism with GA, 3-HGA, and other organic acids typically accumulating in disorders of propionate metabolism, including methylmalonic acid (MMA) and propionic acid (PA) [40]. These effects were evidenced by toxic endpoints such as loss of mitochondrial function, increased production of reactive oxygen species (ROS), and enhanced lipid peroxidation, all of them estimated in freshly prepared rat brain synaptosomal P2/mitochondrial fractions. In addition, we have demonstrated that QUIN is able to enhance toxic endpoints estimated in the striatum of knockout mice for glutaryl-CoA dehydrogenase (*Gcdh*^{-/-}), an *in vivo* transgenic mice model of GA I [41]. Among the markers evaluated, it was found that QUIN stimulated lactate release, reduced the activities of complex IV and creatine kinase, increased lipid and protein oxidation, augmented ROS formation, altered the activities of antioxidant enzymes, and recruited pro-inflammatory signals, all in the striatal tissue of the mutant mice compared with the wild type mice (*Gcdh*^{+/+}). Taken together, the results of these studies support a possible contribution of QUIN to the pathophysiology of GA I during the occurrence of episodes of metabolic decompensation and inflammatory events. However, precise information on how much this toxic synergism affects neuronal cells from the striatum and cortex, and through which mechanisms these damage is produced, is a question that remains unsolved. Therefore, in the present study, we cultured rat neural cells under different experimental conditions (monocultures, co-cultures with astrocytes, and mixed cultures containing neurons + astrocytes + microglia) and exposed them to the presence of QUIN and/or GA in order to establish the precise contribution of this synergic relationship to cell damage and the mechanisms by which the alterations are produced. For this purpose, central components of cell viability [lactate dehydrogenase (LDH) leakage; annexin and propidium iodide (PI) incorporation assays], redox homeostasis [reactive oxygen species (ROS) formation; superoxide dismutase (SOD), catalase (CAT), and glutathione peroxidase (GPx) activities; and the total thiol (-SH) and reduced glutathione (GSH) contents], neuronal plasticity [neurite length and neurite/neuron ratio], and reactive gliosis [glial fibrillary acidic protein (GFAP) increase] were all estimated in the different cultures exposed to QUIN +/- GA for 24 h, thus simulating an acute exposure to these metabolites. Our results reveal that the toxic synergism produced by these molecules augmented cell death, increased ROS formation, and altered antioxidant enzymes activities in different cell cultures, therefore suggesting that oxidative stress might play a major causative role in this new toxic model. These findings are discussed in terms of their relevance for the proposal of a new toxic model for GA I.

Materials and Methods

Reagents

All chemicals were of analytical grade. Phalloidin-fluorescein isothiocyanate (FITC), bis-acrylamide, QUIN, acrylamide, polylysine, anti- β III-tubulin, anti-mouse IgG, anti-mouse IgG-FITC, peroxidase-conjugated anti-mouse IgG, and all reagents for cell culture were obtained from Sigma-Aldrich Co. (St. Louis, MO). 4,6-Diamidino-2-phenylindole (DAPI) was from Calbiochem (La Jolla, CA). Polyclonal glial fibrillary acidic protein (GFAP) antibody was from Dako (Glostrup, Denmark). The enhanced chemiluminescence (ECL) detection kit was from Millipore (Billerica, MA). Anti- β -actin and anti-MAP2 antibodies were from Cell Signaling Technology (Boston, MA). Fetal bovine serum (FBS), Dulbecco's modified Eagle's medium nutrient mixture F-12 (DMEM/F12), Neurobasal medium, B-27 supplement, fungizone, trypsin, and penicillin/streptomycin were purchased from Life Technologies (Carlsbad, CA). All solutions were prepared on the same day of the experiments and the pH was adjusted to 7.2–7.4 in the appropriate buffer for each method.

Ethics Statement

For animal handling, we followed the experimental protocol described in the “Guide for the Care and Use of Laboratory Animals” (NIH publication 85–23, revised 1985). Our protocol was approved by the Ethics Committee for Animal Research of the Universidade Federal do Rio Grande do Sul (No. 18,266). During the experiments, all efforts were made to minimize the number of animals used and their suffering.

Animals

Pregnant Wistar rats (weighing 200–250 g) were obtained from our breeding stock. All rats were kept in 12 h light-dark cycles at a constant temperature (22 °C) in the colony room, with food and water ad libitum. On gestational day 22, animals were constantly observed. At birth, mothers and pups were euthanized by decapitation, and pups were used for astrocyte and microglial cultures. For neuronal cultures, the embryos from mothers euthanized on gestational day 18 were used.

Cell Cultures

Cell cultures were prepared strictly according to the methods previously described by us [42].

Primary astrocyte cultures were obtained and prepared from the striatum and cerebral cortex of newborn (0–1 day old; P0) Wistar rats. The animals were euthanized by

decapitation and their striatum was removed. Dissociated cells were plated in DMEM/F12 supplemented with 10% FBS (pH 7.4), glucose (33 mM), glutamine (2 mM), and sodium bicarbonate (3 mM) in 34.8 and 15.6-mm-diameter wells (six- and 24-well plates; Corning, NY) that had previously been coated with polylysine (1.5 mg/ml; Sigma). Cells were cultured at 37 °C, in a 5% CO₂ atmosphere in a humid incubator, replacing the media every 3 days. An approximate count of 2×10^4 astrocytic cells was seeded on polyornitine-treated coverslips and placed on a 24-well plate, or 2×10^5 astrocytic cells were seeded in a six-well plate. Once astrocytes reached semi-confluence (15 days in vitro; DIV), culture medium was removed and cells were incubated for additional 24 h at 37 °C in a 5% CO₂ atmosphere in DMEM/F12 without FBS, in the presence of 50 μ M QUIN and/or 5 mM GA. Control cultures received the same incubation medium without QUIN or GA. QUIN and GA were prepared prior each treatment and dissolved in DMEM/F12 without FBS. The QUIN concentration employed in this study was established as the half of the concentration needed to alter astrocytic morphology without causing cell death [42]. The GA concentration was established on the basis of previous studies demonstrating moderate or null toxicity in the cerebral cortex of young rats [43].

The striatum and cerebral cortex of 18 Wistar rats at embryonic stage were used to prepare neuronal cell cultures, as previously described [42]. Primary neuronal cell cultures were prepared from the striatum of embryonic (18 days old) Wistar rats, as previously described [44]. For this purpose, pregnant Wistar rats were euthanized, embryos removed, decapitated and their striatum was dissected. Both enzymatic and mechanic digestion consisted of an incubation with 0.05% trypsin for 20 min at 37 °C and further DNase I treatment (0.24 mg/ml in DMEM/F12 supplemented with 10% FBS). Dissociated cells were plated in Neurobasal medium supplemented with 0.5 mM glutamine and B27 supplement (20 ml/l). An approximate number of 5×10^4 neuronal cells were plated on polyornitine-treated coverslips placed on a 24-well plate, or 1.5×10^6 neuronal cells in a six-well plate. Neurobasal medium served to keep neuronal cultures for 24 h; later, culture medium was removed by suction, and cells were incubated for 7 days in a humid incubator (37 °C; 5% CO₂). The neuronal culture medium was replaced at 8 DIV by a medium containing 50 μ M QUIN and/or 5 mM GA. Control cultures received the same incubation medium without QUIN or GA. QUIN and GA were prepared prior each treatment in Neurobasal medium, and control cultures received no QUIN or GA supplementation. The QUIN dose was established on the basis of previous studies [42, 44], and it represents a dose near the one used to alter neuronal morphology without causing cell death. The GA concentration was established on the basis of previous studies demonstrating moderate or null toxicity in the cerebral cortex of young rats [43], yet this and even higher concentrations are found in post mortem brain of GAcidemic

patients during crises of metabolic decompensation frequently occurring during or after inflammatory processes [1, 2].

Primary microglial cultures were obtained from the striatum and cerebral cortex of 1-day-old pups as previously described [42, 45]. Briefly, the striatal tissue of animals was subjected to removal of the meninges and blood vessels, and further triturated. Cells were seeded in DMEM/F12/10% FBS, and 14 DIV after initial seeding, microglial cells were removed from astrocyte monolayer by shaking for 30 min, collected the supernatant, centrifuged, and plated on top of non-related astrocyte monolayers (15 DIV) alone. An estimation of 2×10^4 microglial cells were plated on polyornitine-treated coverslips placed on a 24-well plate, or 2×10^5 microglial cells in a six-well plate.

Freshly obtained and isolated striatal and cortical neurons plated on top of non-related astrocyte monolayers (15 DIV) alone, or non-treated astrocyte monolayers previously associated with microglial cells, served to prepare co-cultures or mixed cultures, respectively. An estimated 5×10^4 neuronal cells were plated on polyornitine-treated coverslips placed on a 24-well plate, or 1.5×10^6 neuronal cells in a six-well plate. Both co-cultures and mixed cultures were kept at 37 °C for 7 days in a humidified 5% CO₂ air atmosphere. When neurons were at 7 DIV, the cultures were used for exposure to QUIN and/or GA for additional 24 h. QUIN and GA were freshly prepared prior each treatment and dissolved in DMEM/F12 without FBS. Control cultures received the same incubation medium without QUIN or GA.

Lactate Dehydrogenase Activity Assay

To evaluate plasma membrane integrity, LDH release was determined by monitoring the leakage of the cytosolic LDH to extracellular medium. Briefly, 20 µl of supernatant, 60 µl potassium phosphate buffer 0.1 M, and 10 µl NADH 1.8 mM was incubated during 5 min. Then, 10 µl pyruvate solution (0.6 mM) was added and LDH was measured spectrophotometrically at 340 nm each 15 s during 4 min, following the rate of conversion of reduced nicotinamide adenine dinucleotide to oxidized nicotinamide adenine nucleotide.

Annexin/Propidium Iodide Assay for Cell Death Estimation

The apoptotic detection assay was carried out by surface labeling with the Ca²⁺-dependent phosphatidylserine-binding protein annexin V. After they had been incubated with the metabolites for 24 h, cells were recovered from the culture plates by 0.05% trypsin-EDTA treatment, centrifuged 1000 rpm for 5 min, and washed once with phosphate-buffered saline (PBS). Cells were labeled by incubation with annexin V-FITC and propidium iodide (PI) in a binding buffer (apoptosis detection kit I-556547; BD Pharmingen) for 15 min

at room temperature in the dark, according to the manufacturer's instruction. Stained cells were acquired (10,000 events) on a FACS Calibur flow cytometer. Analysis was performed in the FlowJo Software.

Oxidative Stress Parameters and Antioxidant Defenses

ROS Formation Assay by 2',7'-Dihydrochlorofluorescein (DCFH) Oxidation

ROS production was measured according to the method of LeBel et al. [46], based on the oxidation of 2'7'-dichlorofluorescein (H₂DCF). The samples were incubated in a medium containing 100 µM H₂DCF-DA solution. Reaction produces the fluorescent compound dichlorofluorescein (DCF) which is measured at $\lambda_{em} = 488$ nm and $\lambda_{ex} = 525$ nm.

Superoxide Dismutase Activity Assay

SOD activity assay is based on the capacity of pyrogallol to autoxidize, a process highly dependent on superoxide, which is a substrate for SOD. The inhibitor of pyrogallol autoxidation occurs in the presence of SOD, whose activity can be then indirectly assayed spectrophotometrically at 420 nm. A calibration curve was performed with purified SOD as a standard, in order to calculate the activity of SOD present in the samples. SOD activity was expressed as the amount of enzyme that inhibits the oxidation of epinephrine by 50%, corresponding to one unit.

Catalase Activity Assay

CAT activity was assayed using SpectraMax M5/M5 Microplate Reader (Molecular Devices, MDS Analytical Technologies, Sunnyvale, CA, USA). This method is based on the disappearance of hydrogen peroxide (H₂O₂) at 240 nm in a reaction medium containing 20 mM H₂O₂, 0.1% Triton X-100, 10 mM potassium phosphate buffer pH 7.0, and 0.1–0.3 mg protein/ml. One CAT unit is defined as 1 mM of H₂O₂ consumed per minute.

Glutathione Peroxidase Activity Assay

GPx activity was measured using *tert*-butyl-hydroperoxide as substrate. NADPH disappearance was monitored at 340 nm using SpectraMax M5/M5 Microplate Reader (Molecular Devices, MDS Analytical Technologies). The medium contained 2 mM GSH, 0.15 U/ml GSH reductase, 0.4 mM sodium azide, 0.5 mM *tert*-butyl-hydroperoxide, and 0.1 mM NADPH. One GPx unit is defined as 1 mM of NADPH consumed per minute, and the specific activity is represented as GPx units/milligram protein.

Sulphydryl Content Assay

This assay was performed as described by Aksenov and Markesbery [47], which is based on the reduction of 5,5'-dithio-bis(2-nitrobenzoic acid) (DTNB) by sulphydryl groups, which in turn, become oxidized (disulfide) generating a yellow derivative (TNB) whose absorption is measured spectrophotometrically at 412 nm. Briefly, 15 μ l of homogenate were added to 275 μ l of phosphate buffer saline pH 7.4 containing 1 mM EDTA. The reaction was started by the addition of 10 μ l of 10 mM DTNB and incubated for 30 min at room temperature in a dark room. The sulphydryl content is inversely correlated to oxidative damage to the protein.

Reduced Glutathione Levels

GSH levels were estimated based on the method described by Browne and Armstrong [48]. Deproteinized samples were mixed to 100 mM sodium phosphate buffer plus 5 mM EDTA. In a dark room, the fluorescent compound (*O*-phthalaldehyde 1 mg/ml diluted in methanol) was added to the media containing the samples. After 15 min, the fluorescence was measured with 420-nm emission and 350-nm excitation. A standard curve was performed using purified GSH. All samples were run in triplicate.

Immunofluorescence Assays for β III-Tubulin, MAP2, and GFAP Detection

Immunocytochemistry was performed as previously described [42]. Briefly, culture cells had been plated on glass coverslips, treated with metabolites for 24 h, and then fixed with 4% paraformaldehyde for 30 min and permeabilized with 0.1% Triton X-100 in PBS for 5 min at room temperature. After having been blocked, cells were incubated overnight with anti- β III-tubulin and anti-MAP2 (for neurons), and anti-GFAP (for astrocytes) at room temperature, followed by PBS washes and incubation with specific secondary antibody conjugated with Cy3 (sheep anti-rabbit) or with FITC (sheep anti-mouse) for 1 h. In each immunostaining experiment, negative controls were performed by omitting the primary antibody. In controls, no reactivity was observed. The nucleus was stained with 4',6-diamidino-2-phenylindole (DAPI) (0.25 mg/ml). Cells were visualized with a Nikon inverted microscope, and images were transferred to a computer with a digital camera (Sound Vision).

Morphometric Analysis

For neurons, the neurite/neuron ratio and the neurite length were analyzed in ImageJ (NIH) as previously described [42]. The number of processes originating from the soma was measured manually, and all neurites emerging from neuronal soma were considered. To measure the neurite length, we used an

ImageJ plug-in that allows semiautomatic tracing of neuritis for measurements of neurite length. Neurite length was analyzed by considering only the major process of each neuron.

The cytoplasmic area of astrocytes stained for GFAP cytoskeleton was measured in ImageJ and used as a criterion for morphological alteration. An ImageJ plug-in that allows semiautomatic tracing of the area of interest was used to measure the cytoplasmic area. Four independent experiments were performed in triplicate, encompassing 10 fields randomly chosen in each group. The data were stored and morphometric analyses were carried out in GraphPad Prism 5.

Statistical Analysis

Results are presented as mean \pm standard deviation. Assays were performed in triplicate and the mean was used for statistical calculations. Quadruplicate experiments were always carried out and the mean used for the calculations. Results were statistically analyzed with two-way ANOVA followed by Bonferroni's post hoc test. Statistical analysis was performed with the GraphPad 5.0 software. Differences were considered significant when $P \leq 0.05$.

Results

Co-administration of QUIN and GA Increased Cell Damage in Striatal and Cortical Cultures and Decreased Viability in Striatal Neurons

We first evaluated the effect of the QUIN + GA co-incubation on LDH release and viability through the annexin and propidium iodide assay in neuronal cultures (Fig. 1a, d), co-cultures (Fig. 1b, e), and mixed cultures (Fig. 1c, f) from the rat striatum (Fig. 1a–c) and cortex (Fig. 1d–f). LDH activity was increased in the QUIN + GA condition (compared to control values) in striatal (Fig. 1a, $P < 0.001$) and cortical (Fig. 1d, $P < 0.01$) neuronal cultures, as well as in cortical mixed cultures ($P < 0.05$).

Interestingly, striatal cultures seem to be more sensitive to GA, since in all cell types there was an increase in LDH release when cultures were treated with this metabolite (Fig. 1a–c, $P < 0.001$). However, in cortical cultures, additive or synergic effects of both toxins were observed in neuronal and mixed cultures ($P < 0.01$), except for the case of co-cultures.

Next, we evaluated the type of cell death triggered by QUIN and GA in primary neurons using the annexin-PI assay. We found a decreased number of live striatal neurons in all treated groups (Fig. 1g, $P < 0.001$) compared to control cultures, where the percent values of cells in early apoptosis, late apoptosis, and necrosis were significantly increased by the QUIN + GA treatment compared to the all other treatments (Fig. 1g, $P < 0.001$). No changes in these parameters were observed in cortical cultures (Fig. 1h).

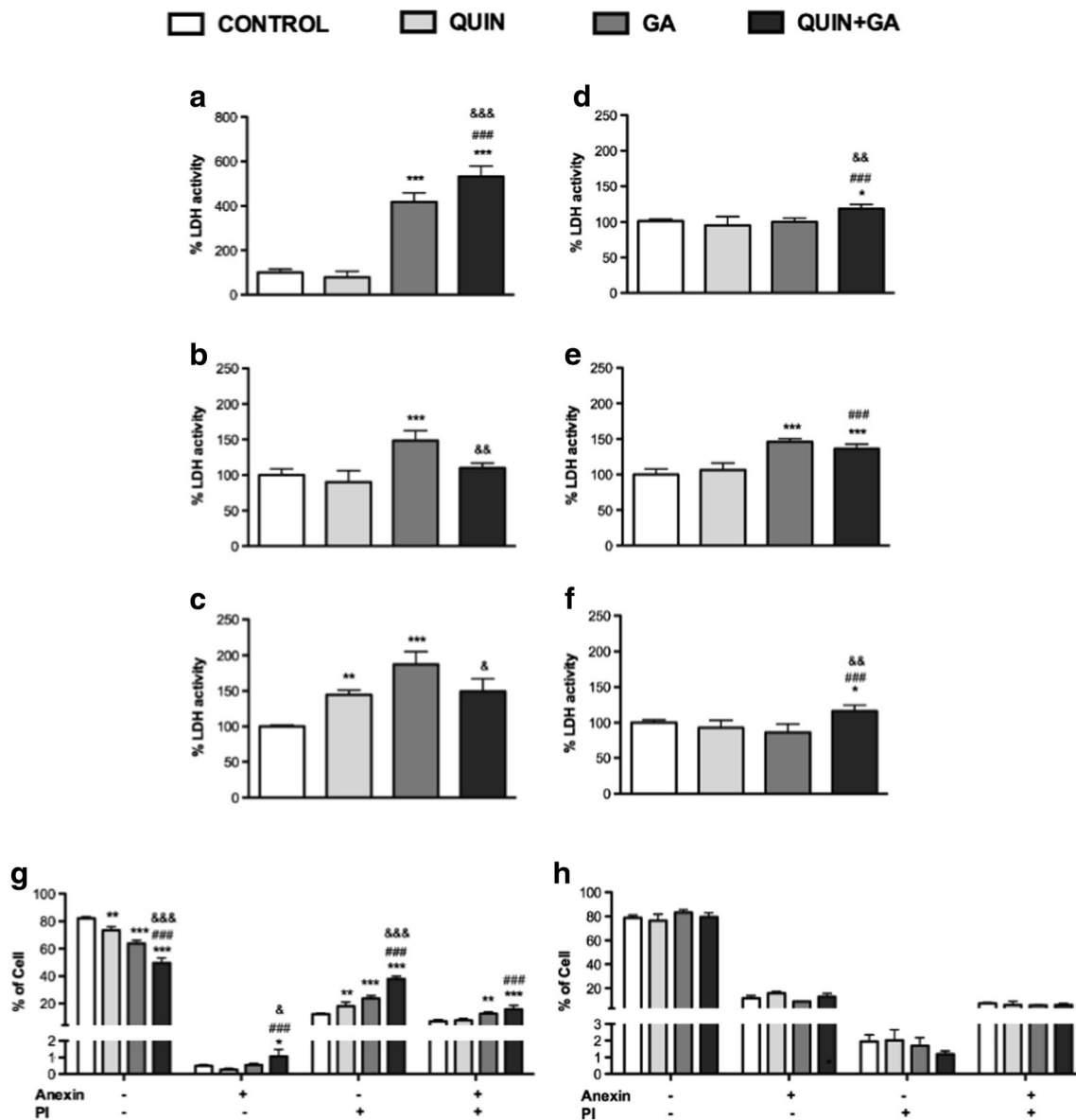


Fig. 1 Effects of QUIN and/or GA on cell viability and damage of neurons, co-cultures (astrocyte and neurons), and mixed cultures (neurons, astrocytes, and microglia). Cells were treated with QUIN (50 μ M) and/or GA (5 mM) for 24 h (8 DIV), and cell damage was assessed as LDH activity. Results of striatal cultures are shown in **a** (neurons), **b** (co-cultures), and **c** (mixed cultures). Results of cortical cultures are shown in **d** (neurons), **e** (co-cultures),

and **f** (mixed cultures). Viability of striatal (**g**) and cortical (**h**) neurons was measured by annexin V-FITC and PI assays. Data are reported as mean \pm SD of four independent experiments performed in triplicate. Results were statistically analyzed by two-way ANOVA followed by Bonferroni's post hoc test. ** $P < 0.01$ and *** $P < 0.001$, different of control; #### $P < 0.0001$, different of QUIN; & $P < 0.05$, && $P < 0.01$, and &&& $P < 0.001$, different of GA

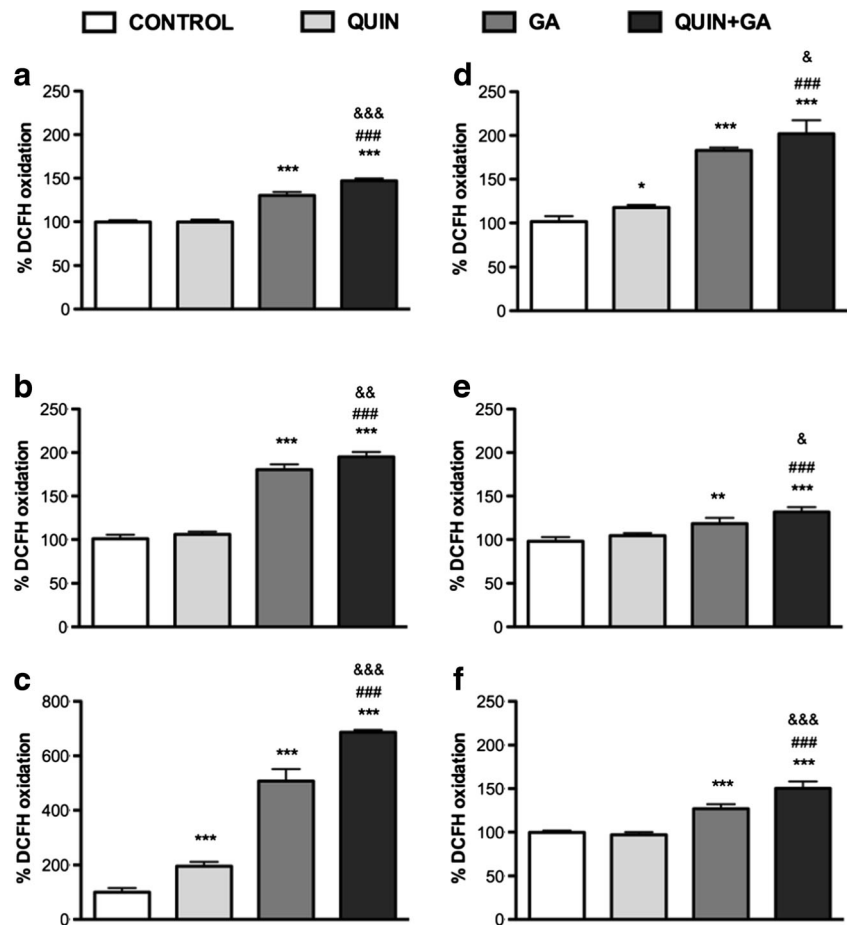
QUIN + GA Treatment Increased ROS Formation in Striatal and Cortical Neuronal Cultures, Co-cultures, and Mixed Cultures

The percent levels of ROS formation in neuronal cultures (Fig. 2a, d), co-cultures (Fig. 2b, e), and mixed cultures (Fig. 2c, f) exposed to QUIN + GA are presented in Fig. 2. ROS formation in all striatal (Fig. 2a–c) and cortical (Fig. 2d–f) cultures was significantly increased ($P < 0.001$) by the QUIN + GA treatment compared to control, QUIN, and GA conditions.

QUIN + GA Condition Decreased SOD Activity and Increased CAT Activity in Striatal Cultures

Figure 3 depicts the effects of QUIN, GA, and QUIN + GA on SOD activity (Fig. 3a, f, k), CAT activity (Fig. 3b, g, l), GPx activity (Fig. 3c, h, m), -SH groups content (Fig. 3d, i, n), and GSH content (Fig. 3e, j, o) in striatal neuronal cultures (Fig. 3a–e), co-cultures (Fig. 3f–j), and mixed cultures (Fig. 3k–o). The QUIN + GA condition decreased the levels of SOD activity compared to control, QUIN, and GA treatments in neuronal cultures ($P < 0.001$), co-cultures ($P < 0.01$), and mixed cultures

Fig. 2 Effects of QUIN and/or GA on 2',7'-dihydrodichlorofluorescein (DCFH) oxidation (reactive oxygen species (ROS) formation) in neurons, co-cultures (astrocyte and neurons), and mixed cultures (neurons, astrocytes, and microglia). Cells were treated with QUIN (50 μ M) and GA (5 mM) for 24 h (8 DIV). Results of striatal cultures are shown in **a** (neurons), **b** (co-cultures), and **c** (mixed cultures). Results of cortical cultures are shown in **d** (neurons), **e** (co-cultures), and **f** (mixed cultures). Data are reported as mean \pm SD of four independent experiments performed in triplicate. Results were statistically analyzed by two-way ANOVA followed by Bonferroni's post hoc test. * $P < 0.05$, ** $P < 0.01$, and *** $P < 0.001$, different of control; ### $P < 0.001$, different of QUIN; & $P < 0.05$, && $P < 0.01$, and &&& $P < 0.001$, different of GA



($P < 0.001$). In contrast, CAT activity levels were significantly increased in neuronal cultures ($P < 0.001$) and co-cultures ($P < 0.01$) and decreased in mixed cultures ($P < 0.001$). Significant changes on other parameters induced by QUIN + GA treatment compared to other treatments, included an increase in GPx activity in co-cultures ($P < 0.01$), a depletion of -SH groups in neuronal cultures and co-cultures ($P < 0.001$), and a decrease in GSH levels in neuronal cultures ($P < 0.01$).

QUIN + GA Treatment Decreased SOD Activity and GSH Levels in Cortical Cultured Neurons

The effects of QUIN, GA, and QUIN + GA on the cortical SOD activity (Fig. 4a, f, k), CAT activity (Fig. 4b, g, l), GPx activity (Fig. 4c, h, m), -SH groups content (Fig. 4d, i, o), and GSH content (Fig. 4e, j, p) in cortical neuronal cultures (Fig. 4a–e), co-cultures (Fig. 4f–j), and mixed cultures (Fig. 4k–p) are shown in Fig. 4. When cells were treated with QUIN + GA, the levels of SOD were decreased in neuronal cultures ($P < 0.001$) and co-cultures ($P < 0.01$) compared to control, QUIN, and GA treatments. In addition, QUIN + GA condition also depleted the levels of GSH in neuronal cultures ($P < 0.01$) and mixed cultures ($P < 0.001$) compared to all other treatments. No changes in other parameters were observed.

QUIN + GA Condition Did Not Potentiate the Decrease in Neurite/Neuron Ratio, Neither the Neurite Length in Cortical Cultures Exposed to QUIN or GA

Since neuronal cultures were more susceptible to the QUIN + GA than any other cell culture studied, two endpoints of neurite development were estimated in cortical neurons: neurite/neuron ratio and neurite length after labeling cells with MAP2 (Fig. 5). For both markers, the QUIN + GA treatment did not exert any additive toxic effect compared to the toxins alone. In turn, while QUIN exerted a prominent decrease in both the neurite/neuron ratio and the neurite length ($P < 0.001$) compared to control, GA produced a less intense effect on both markers ($P < 0.01$).

QUIN + GA Condition Did Not Potentiate Reactive Gliosis, Neither Affected the Neurite/Neuron Ratio Nor the Neurite Length in Cortical Co-cultures

Figure 6 depicts the effects of QUIN and/or GA on astrocytic cytoplasmic area as an index of reactive gliosis in cortical co-cultures. The neurite/neuron ratio and the neurite length are also shown as indexes of the physiological status of neuronal cells. Immunocytochemical results (in Fig. 6a) from astrocytes

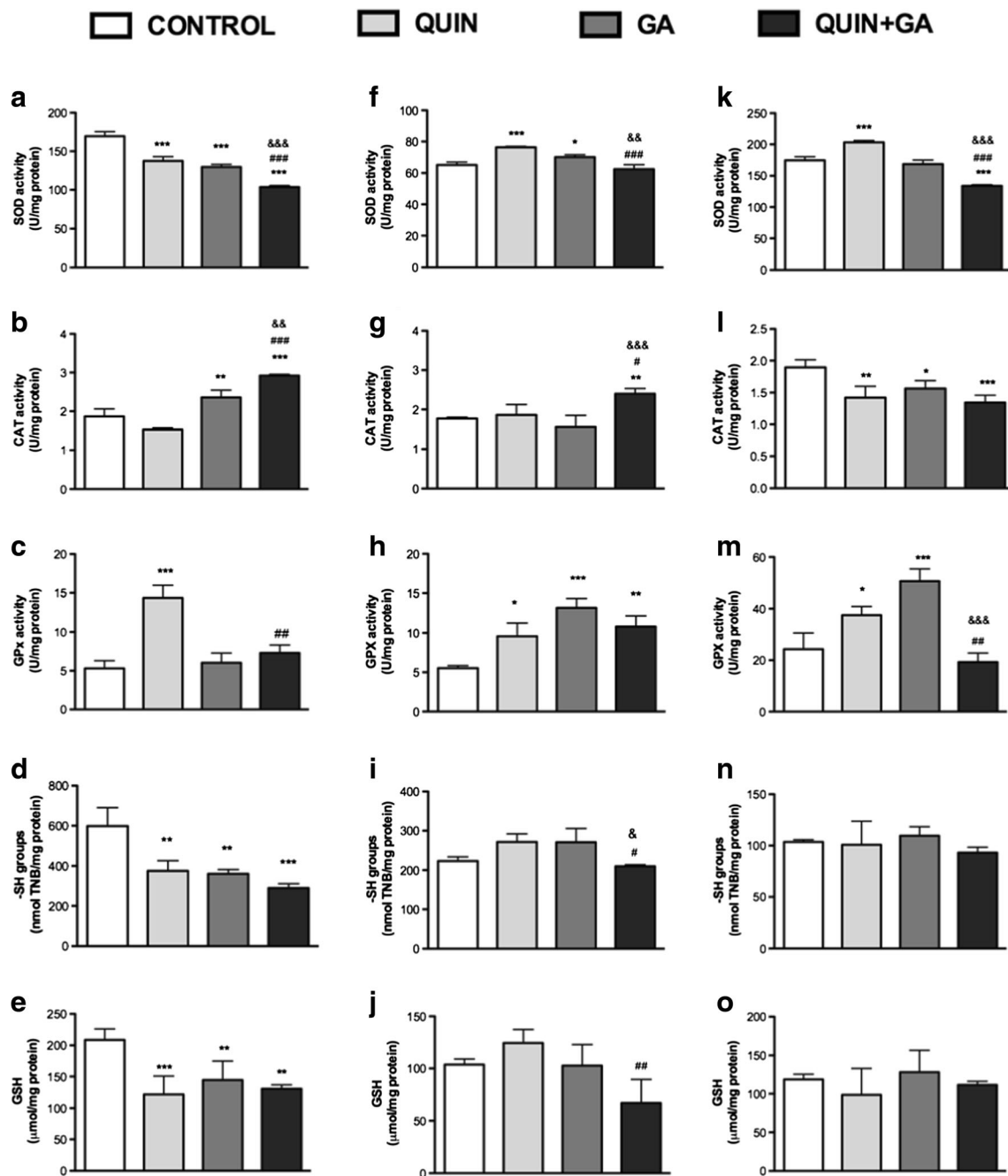


Fig. 3 Effects of QUIN and/or GA on antioxidant enzyme activity, GSH levels and -SH groups in striatal cell cultures. Cells were treated with QUIN (50 μ M) and GA (5 mM) for 24 h (8 DIV). Results of cultured neurons (a–e), co-cultures (f–j), and mixed cultures (k–o) are shown. Data are reported as mean \pm SD of four independent experiments performed in triplicate. Results

were statistically analyzed by two-way ANOVA followed by Bonferroni's post hoc test. * P < 0.05, ** P < 0.01, and *** P < 0.001, different of control; # P < 0.05, ## P < 0.01, and ### P < 0.001, different of QUIN; & P < 0.05, && P < 0.01, and &&& P < 0.001, different of GA

labeled with GFAP and neuronal cells labeled with MAP2 showed no additive effects for the QUIN + GA condition compared to the effects of the toxins alone. QUIN, but not GA, was able to increase reactive gliosis in a significant manner (P < 0.001) compared to control (Fig. 6d). Neither the neurite/neuronal ratio (Fig. 6b) nor the neurite length (Fig. 6c) was affected by QUIN and/or GA in co-cultures.

MK-801 and Melatonin Decreased the Cell Damage Induced by QUIN + GA in Striatal Neurons, but Only Melatonin Prevented ROS Formation and Loss of Cell Viability

Figure 7 shows the effects of the well-known NMDAR antagonist MK-801, and the broad-spectrum antioxidant

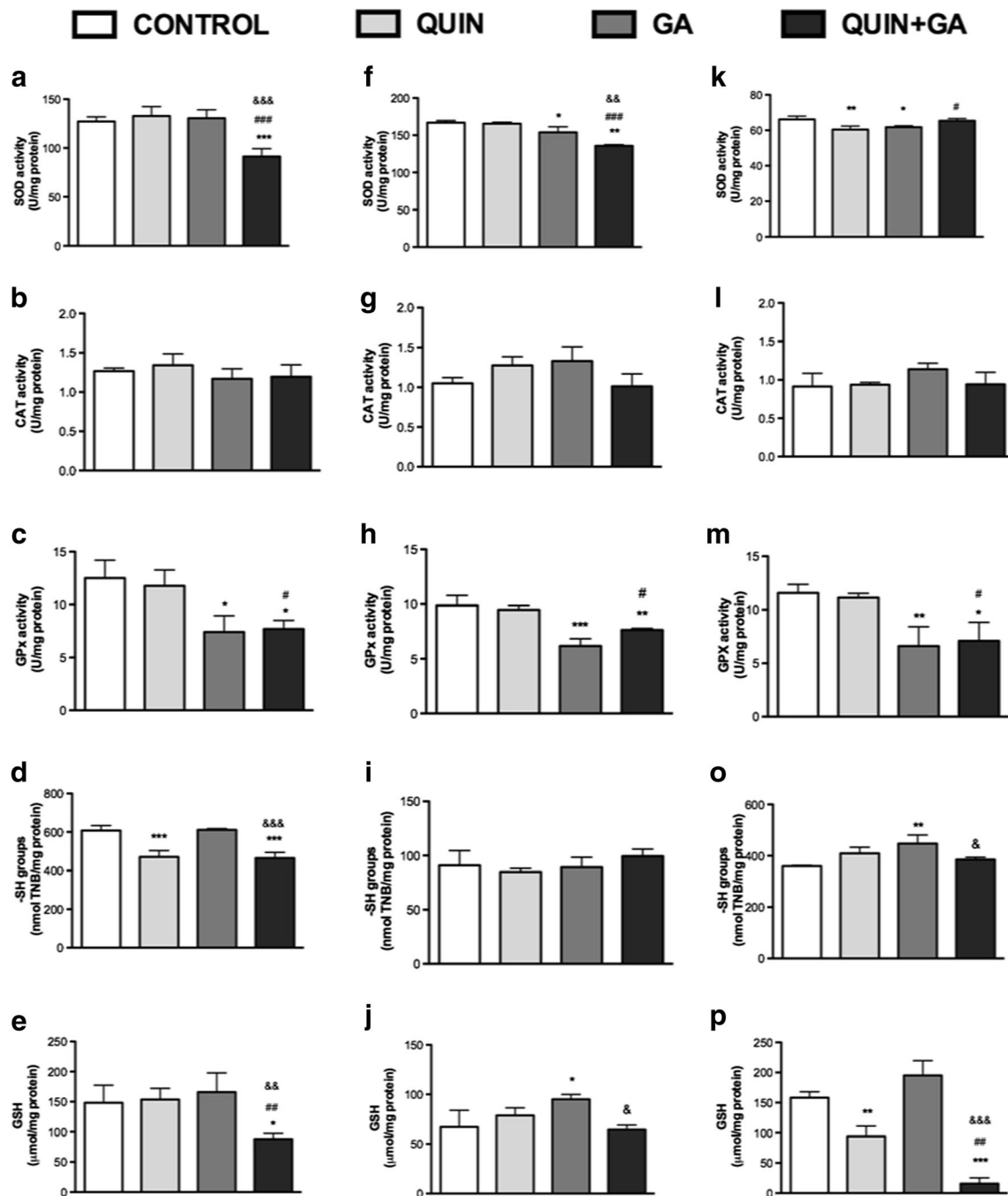


Fig. 4 Effects of QUIN and/or GA on antioxidant enzyme activity, GSH levels and -SH groups content in cortical cell cultures. Cells were treated with QUIN (50 μ M) and GA (5 mM) for 24 h (8 DIV). Results of cultured neurons (a–e), co-cultures (f–j), and mixed cultures (k–p) are shown. Data are reported as mean \pm SD of four independent experiment performed in

triplicate. Results were statistically analyzed by two-way ANOVA followed by Bonferroni's post hoc test. * P < 0.05, ** P < 0.01, and *** P < 0.001, different of control; # P < 0.05, ## P < 0.01, and ### P < 0.001, different of QUIN; & P < 0.05, && P < 0.01, and &&& P < 0.001, different of GA

melatonin, on the cell damage and loss of viability induced by the QUIN + GA condition in cultured striatal neurons. Exposure of neuronal cells to QUIN + GA provoked a significant increase in LDH leakage (70–98%; P < 0.05–0.01; Fig. 7a, b) and ROS formation (53–121%; P < 0.01–0.001) compared to the control (Fig.

7c, d). MK-801 only reduced the QUIN + GA-induced cell damage (65% below QUIN + GA; P < 0.001; Fig. 7a). In contrast, melatonin decreased both the LDH activity (58% below; P < 0.01) and ROS formation (32% below; P < 0.001) induced by the QUIN + GA condition (Fig. 7b, d, respectively).

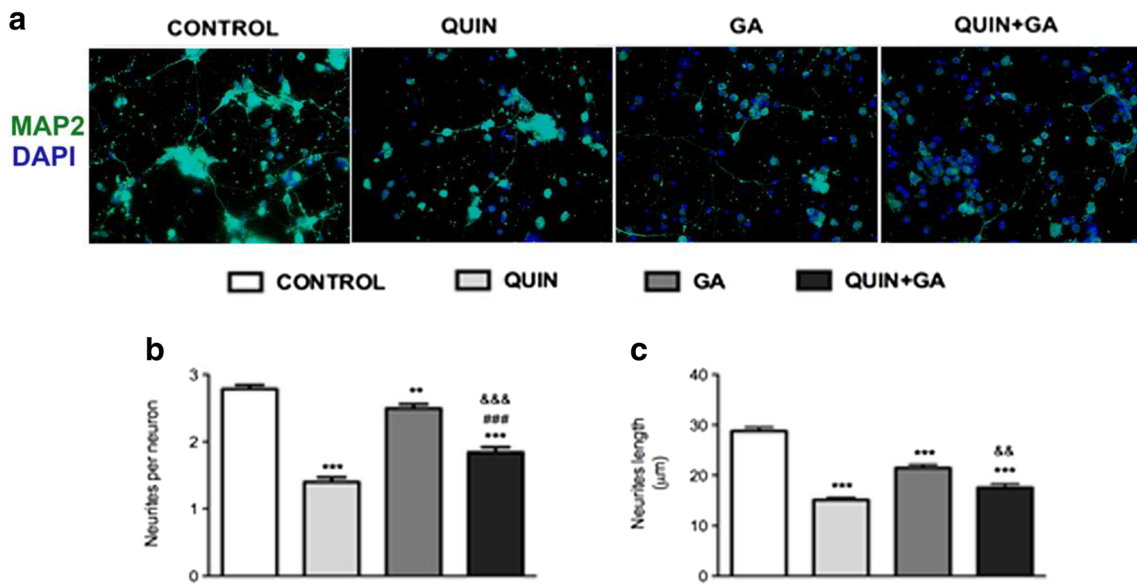


Fig. 5 Effects of QUIN and/or GA on the neurite length and the neurite/neuron ratio in cultured cortical neurons. Cells were treated with QUIN (50 µM) and GA (5 mM) for 24 h (8 DIV). **a** Representative images of cells immunostained with anti-MAP2 (green) antibodies and DAPI for nuclei (blue). **b** Graphical representation of the neurite/neuron ratio. **c** Graphical representation of neurite length. Data are reported as mean

values ± standard error of four independent experiments, considering 10 fields randomly chosen from each group. Results were statistically analyzed by two-way ANOVA followed by Bonferroni’s post hoc test. ** $P < 0.01$ and *** $P < 0.001$, different of control; ### $P < 0.001$, different of QUIN; && $P < 0.01$ and &&& $P < 0.001$, different of GA

In regard to the assay to determine the type of cell death produced by the QUIN + GA treatment in primary striatal neurons by the annexin-PI assay (Fig. 7e), for this series of experiments, we found that this treatment decreased the number of living cells by 18% compared to control ($P < 0.001$) and increased the number of cells in

early apoptosis by ~20% ($P < 0.001$), in late apoptosis by ~15% ($P < 0.001$), and in necrosis by ~14% ($P < 0.01$). Melatonin was able to prevent the loss of living cells and the increase in the number of cells in apoptosis and necrosis ($P < 0.05$). Melatonin per se produced no effects on these parameters.

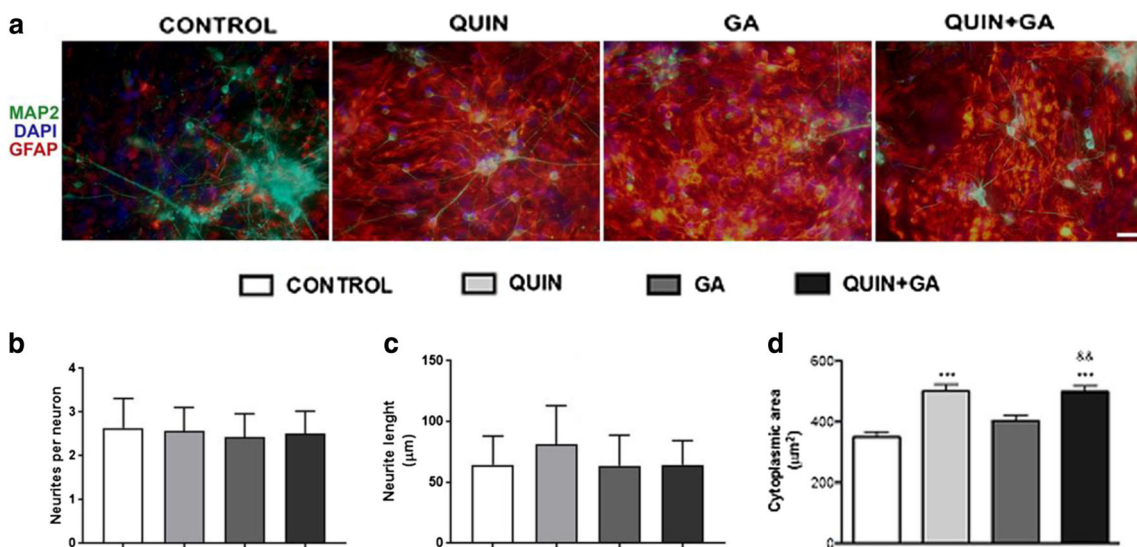
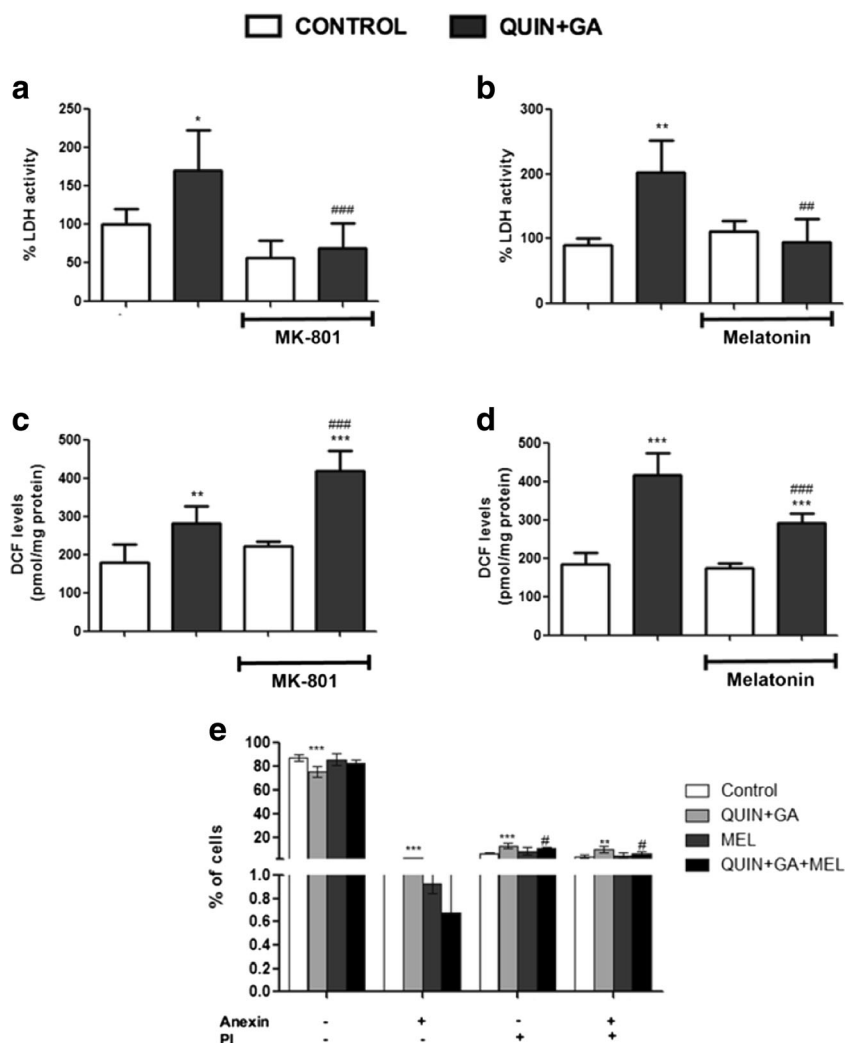


Fig. 6 Effects of QUIN and/or GA on astrocytic and neuronal morphology. Cells in cortical co-culture were treated with QUIN (50 µM) and GA (5 mM) for 24 h (8 DIV). **a** Representative images of astrocytes immunostained with anti-GFAP (red), neurons immunostained with MAP2 (green), and DAPI (blue) are shown. Effect of QUIN and GA on neurite per neuron (**b**), neurite length (**c**), and cytoplasmic area of astrocytes (**d**).

Data are reported as mean ± standard error of four independent experiments, considering 10 fields randomly chosen from each group. Results were statistically analyzed by two-way ANOVA followed by Bonferroni’s post hoc test. *** $P < 0.001$, different of control; && $P < 0.01$, different of GA

Fig. 7 Protection against QUIN + GA-induced cell death and ROS production. Striatal neurons were preincubated with the glutamate antagonist MK-801 (a, c) and the antioxidant melatonin (b, d, e) for 1 h before QUIN + GA treatment for 24 h as described in the “Materials and Methods” section. Data are reported as mean \pm SD of four independent experiments performed in triplicate. Results were statistically analyzed by two-way ANOVA followed by Bonferroni’s post hoc test. * $P < 0.05$, ** $P < 0.01$, and *** $P < 0.001$, different of control; # $P < 0.05$, ## $P < 0.01$, and ### $P < 0.001$, different of QUIN + GA



Discussion

In the present study, we provide evidence demonstrating that simultaneous addition of QUIN and GA to primary striatal and cortical cultures led to alterations in redox homeostasis and cell death. We have also shown a differential susceptibility of neurons, co-cultures, and mixed cultures to these metabolites.

Exposure of primary striatal neurons with either GA or QUIN independently induced neuronal death, as observed in the experiments with annexin-PI. However, when combined, these two metabolites exerted synergistic and differential toxic effects leading to cell death, triggering both apoptotic and necrotic mechanisms. Evidence of this synergistic actions exerted by the combined presence of QUIN + GA has been reported by us both in in vitro—in brain synaptosomes—[40] and in vivo—in glutaryl-CoA dehydrogenase KO mice—[41] conditions.

Certain neurotoxins can induce both apoptosis and necrosis, depending on the toxic conditions and pathways they stimulate, particularly regarding redox levels and

mitochondrial integrity. This consideration is consistent with the fact that the signaling pathways involved in the different types of cell death can sometimes overlap and are engaged in response to specific stimuli [49]. In line with this, glutamate can induce either early necrosis or delayed apoptosis in cultures of cerebellar granule cells, wherein the mitochondrial function is a critical factor that determines the mode of neuronal death in excitotoxicity [50]. Moreover, the maintenance of mitochondrial function may therefore be a decisive factor in determining the degree and progression of neuronal injury caused by excitotoxins. Therefore, an increase in cytosolic calcium triggered by excitotoxins like QUIN and GA is critical for mitochondrial dysfunction, causing oxidative stress [51] and nNOS activation and affecting the mitochondrial membrane potential.

Oxidative stress represents a critical event related with QUIN and GA neurotoxicity [15, 20]. Accordingly, we found that ROS generation and depleted antioxidant defenses take part on the QUIN + GA-induced cytotoxicity of QUIN + GA in neuronal cells. When investigating SOD, CAT, and GPx

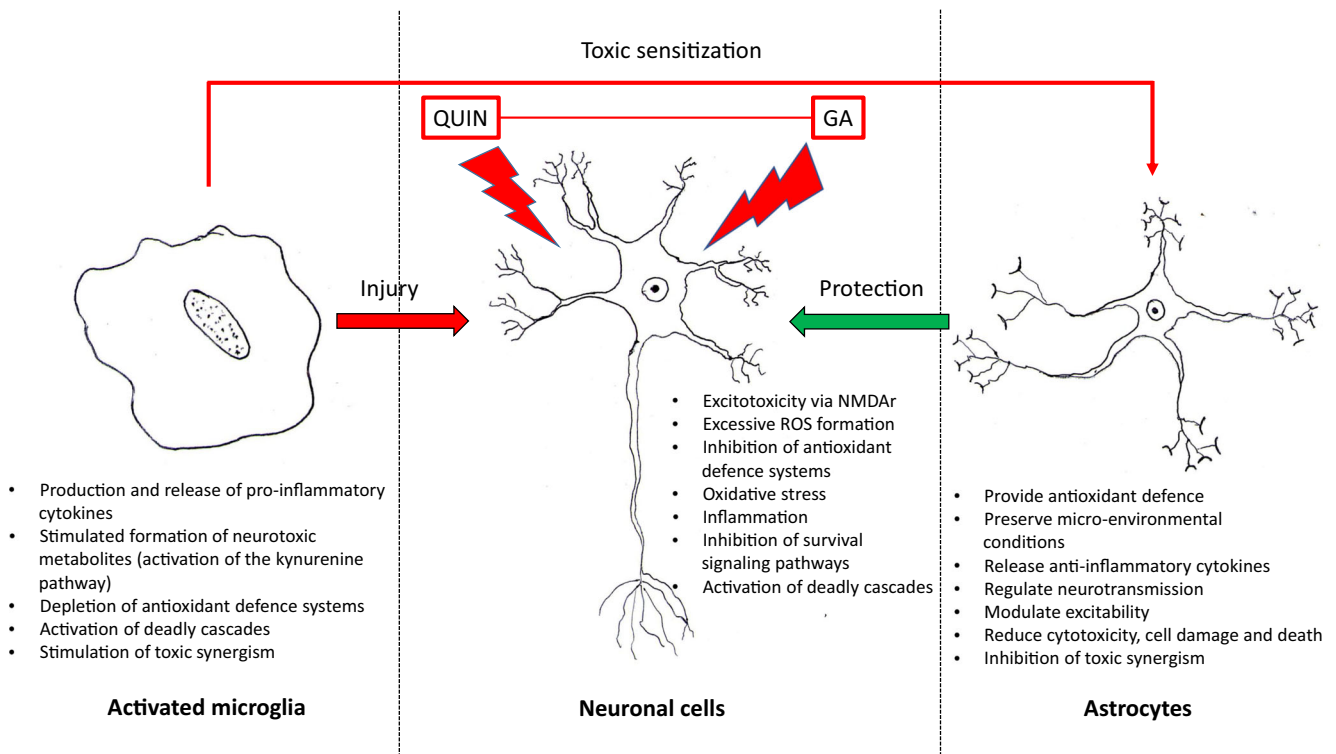


Fig. 8 Schematic representation of hypothetical mechanisms involved in the toxic pattern triggered by quinolinic acid (QUIN) + glutamic acid (GA) in striatal and cortical neuronal cell cultures, co-cultures (neuronal cells plus astrocytes), and mixed cultures (neuronal cells plus astrocytes plus microglia) from the rat brain. In the center, neuronal cells are directly attacked by QUIN + GA via overstimulation of *N*-methyl-D-aspartate receptor (NMDAR) and/or oxidative stress. These effects will trigger damaging cell pathways while silencing survival signals, leading to cell death produced by toxic synergism. When neuronal cells are co-incubated with astrocytes (right box), the defense systems of the later help to protect

neuronal cells by providing them antioxidant and anti-inflammatory assistance, reducing excitability, and stimulating survival signaling pathways. In turn, when neuronal cells are co-incubated with astrocytes and activated microglia (left box), the toxic responses affecting neuronal cells exposed to QUIN + GA prevail and are stimulated by damaging signals produced by microglia, including pro-inflammatory responses, loss of antioxidant potency, and activation of deadly cascades; thus, microglia could silence the positive effects of astrocytes in the QUIN + GA toxic paradigm

activities, representing the main antioxidant enzymes for the detoxification of reactive species [52], we found diminished SOD and increased CAT activities in striatal neurons, and diminished SOD activity and GSH levels in cortical neurons, together with diminished GSH content and SH groups. In line with this, the antioxidant melatonin, but not the NMDAR antagonist MK-801, was able to prevent both ROS production and LDH release and diminished the number of viable striatal neurons, suggesting that oxidative stress is associated with neuronal death in the combined QUIN + GA toxic pattern.

GSH is the most prevalent cellular thiol that plays an essential role in preserving a reduced intracellular environment, protecting DNA, proteins, and lipids against oxidation. Furthermore, GSH depletion by ROS and RNS is a central signaling event that regulates the activation of cell death pathways in distinct pathologies, such as in common neurodegenerative disorders, cancer, and autoimmunity [53]. Herein, we found depletion in the GSH content in striatal and cortical neurons treated with the toxic metabolites, suggesting that GSH depletion is part of the mechanisms by which QUIN + GA trigger neuronal death. However, it is important to note

that, as abovementioned, although melatonin could prevent both cell death and ROS production in striatal neurons, the NMDA antagonist MK-801 was able to prevent only LDH release. These findings suggest that other mechanisms are involved in the neuronal death triggered by QUIN and GA beyond ROS production and excitotoxicity. In line with this, melatonin is known to antagonize both excitotoxicity and mitochondrial dysfunction [54, 55]. Consistently, NMDA-induced calcium rises were diminished by melatonin in cultured mouse striatal neurons [56], also inhibiting nNOS [57]. Moreover, anti-apoptotic effects of melatonin have been described in numerous publications and summarized in several reviews [58–61], in which it has been demonstrated that this antioxidant acts directly on membrane potential as well as on the mitochondrial permeability transition pore [56]. Therefore, our results suggest that, despite that QUIN + GA model exerts its effect in part by NMDAR overactivation, which would increase the cytosolic calcium, affect mitochondrial function, and trigger mechanisms of apoptotic and necrotic cell death, other mechanisms cannot be discarded. It is important to note that despite QUIN damage to neural cells is greatly ascribed to

NMDA-mediated excitotoxicity in several brain areas, our present results suggest that cell death in striatal cultures is through mechanisms not disturbed by NMDA antagonist MK-801. Although further studies with silenced or dysfunctional NMDA receptors will be necessary to assume that QUIN + GA effects are completely dissociated from NMDA receptors, our present findings suggest that, at least in our *in vitro* conditions, QUIN + GA toxicity is mediated by other mechanisms beyond NMDA receptor. Moreover, studies showed that QUIN actions also involve metabotropic glutamate receptors and Ca^{2+} release from intracellular stores besides Ca^{2+} influx through NMDA receptors [44, 62]. In this line, it has been shown that QUIN can produce oxidative damage independent of its activity under NMDA receptor [63]. The evidence collected herein also demonstrates that the QUIN + GA condition induces a synergic action on cell dysfunction and death, supporting a coordinated mechanism of toxicity for these two agents.

Of note, in co-cultures, QUIN + GA did not exert any synergistic effect on LDH release as compared to GA alone. Indeed, GA alone exerted a prominent increase in LDH release in striatal co-culture, while QUIN + GA had no effect on this parameter. Although both metabolites are able to alter the redox homeostasis and increase ROS production in striatal and cortical co-cultures, these effects seem not to be associated with the cell death observed.

Our results showing no cell death in striatal co-cultures suggest that the neuron-astrocyte interaction could prevent cell death caused by the metabolites. Accordingly, a recent study with striatal co-cultures treated with QUIN showed that the metabolite activates FGF2/Erk signaling, preventing neuronal and astrocytic cytoskeletal disruption and ROS production [42]. This effect might be inherent also to GA. On the other hand, in cortical co-cultures, QUIN + GA caused a decrease in SOD and GPx activity, with an increase in ROS production and concomitant cell death. In turn, this effect highlights different mechanisms triggered by the metabolites on striatal or cortical cells, supporting regional susceptibilities to toxic insults.

Contrariwise, when mixed cultures were treated with QUIN + GA, a potentiating effect of the two metabolites was observed. The results showed a diminished SOD and CAT in striatal mixed cultures and diminished SOD, GPx activities, and GSH content in cortical mixed cultures. This imbalance resulted in increased ROS production and cell death in both striatal and cortical cells. These results demonstrate a role of microglial cells on the effects triggered by the metabolites, especially in striatal cultures, since we did not observe cell death when microglial cells are not present.

Microglia can respond to injury, ischemia, infection, or inflammation in the CNS with morphological modifications, activation and expression of membrane receptors, and secretion of pro-inflammatory cytokines or mediators like ROS and RNS [64, 65]. These findings could explain, at least in part,

why the symptomatology of patients with GA I is worsened during infections or immunization. During these scenarios, microglia can be activated and secrete QUIN, which in turn induces more microglial activation, with the consequent ROS production and cell death. According to our study, the role of microglia in the cell death triggered by the metabolites seems to be more prominent in striatal cells. This is in line with striatal damage observed in GA I patients and could explain, at least in part, the degeneration associated with infections, fever, or prolonged fasting.

Compared with glutamate or NMDA, the extent of neuronal damage caused by GA alone is weak. Therefore, it is suggested that additional amplifying factors are necessary to explain the neurodegeneration seen in the disease. The hypothesis that QUIN may be involved in the neuropathology of GA I started in 1987 [13]. This hypothesis stated that deficiency of glutaryl-CoA dehydrogenase blocks the glutarate pathway, and this could activate the first enzyme of kynurenine pathway in macrophages and microglia, especially during inflammatory processes, leading to overproduction of QUIN. Consequently, synergistic effect of these two metabolites, which alone does not have sufficient toxic potency, may be involved in the pathogenesis of striatal degeneration.

In summary, our results, together with previous reports in literature demonstrating synergic toxic actions of QUIN + GA in rat brain synaptosomes [40], as well as in the mutant mice model of GA I produced by deletion of GCDH [41], support the existence of cooperative mechanisms elicited by these two metabolites to potentiate neuronal cell damage in a process that is not only relevant for GA I but also for other neurological disorders with excitotoxic, pro-oxidant, pro-inflammatory, and degenerative components. Finally, Fig. 8 summarizes the mechanisms proposed to occur in cells exposed to the QUIN + GA condition and the role that NMDAr blockade and the induction of oxidative damage play in this model.

Acknowledgements We are grateful to the financial support of CNPq, PROPESq/UFRGS, FAPERGS, PRONEX, FINEP Rede Instituto Brasileiro de Neurociência (IBN-Net) # 01.06.0842-00, and Instituto Nacional de Ciência e Tecnologia-Excitotoxicidade e Neuroproteção (INCT-EN).

Author Contributions Conceived and designed the experiments: PP, ALCG, AW, MW, and AS. Performed the experiments and analyzed the data: PP, ALCG, HB, and JCS. Wrote the paper: PP, MW, and AS. Funding This work was supported by CNPq, PROPESq/UFRGS, FAPERGS, PRONEX, FINEP Rede Instituto Brasileiro de Neurociência (IBN-Net) # 01.06.0842-00, and Instituto Nacional de Ciência e Tecnologia-Excitotoxicidade e Neuroproteção (INCT-EN).

Compliance with Ethical Standards

Conflict of Interest The authors declare that they have no conflict of interest.

Research Involving Animals For animal handling, we followed the experimental protocol described in the “Guide for the Care and Use of Laboratory Animals” (NIH publication 85–23, revised 1985). Our protocol was approved by the Ethics Committee for Animal Research of the Universidade Federal do Rio Grande do Sul (No. 18,266). During the experiments, all efforts were made to minimize the number of animals used and their suffering.

References

1. Brismar J, Ozand PT (1995) CT and MR of the brain in glutaric aciduria type I: a review of 59 published cases and a report of 5 new patients. *Am J Neuroradiol* 16:675–683
2. Goodman S, Fremman F (2001) Organic acidemias due to defects in lysine oxidation: 2-ketoadipic acidemia and glutaric acidemia. In: Scriver CR, Beaudet AL, Sly WS, Valle D (eds) *The metabolic and molecular bases of inherited disease*. McGraw-Hill Inc., New York, pp. 2195–2204
3. Goodman SI, Norenberg MD, Shikes RH, Breslich DJ, Moe PG (1977) Glutaric aciduria: biochemical and morphologic considerations. *J Pediatr* 90:746–750
4. Heringer J, Boy SP, Ensenauer R, Assmann B, Zschocke J, Harting I, Lücke T, Maier EM et al (2010) Use of guidelines improves the neurological outcome in glutaric aciduria type I. *Ann Neurol* 68:743–752
5. Hoffmann GF, Zschocke J (1999) Glutaric aciduria type I: from clinical, biochemical and molecular diversity to successful therapy. *J Inher Metab Dis* 22:381–391
6. Kölker S, Sauer SW, Hoffmann GF, Müller I, Morath MA, Okun JG (2008) Pathogenesis of CNS involvement in disorders of amino and organic acid metabolism. *J Inher Metab Dis* 31:194–204
7. Hensley K, Mhatre M, Mou S, Pye QN, Stewart C, West M, Williamson KS (2006) On the relation of oxidative stress to neuroinflammation: lessons learned from the G93A-SOD1 mouse model of amyotrophic lateral sclerosis. *Antioxid Redox Signal* 8:2075–2087
8. Hunter RL, Dragicevic N, Seifert K, Choi DY, Liu M, Kim HC, Cass WA, Sullivan PG et al (2007) Inflammation induces mitochondrial dysfunction and dopaminergic neurodegeneration in the nigrostriatal system. *J Neurochem* 100:1375–1386
9. Tilleux S, Hermans E (2007) Neuroinflammation and regulation of glial glutamate uptake in neurological disorders. *J Neurosci Res* 85:2059–2070
10. Muhl H, Pfeilschifter J (2003) Endothelial nitric oxide synthase: a determinant of TNF α production by human monocytes/macrophages. *Biochem Biophys Res Commun* 310:677–680
11. Maddison DC, Giorgini F (2015) The kynurenine pathway and neurodegenerative disease. *Semin Cell Dev Biol* 40:134–141
12. Schwarcz R, Bruno JP, Muchowski PJ, Wu HQ (2012) Kynurenines in the mammalian brain: when physiology meets pathology. *Nat Rev Neurosci* 13:465–477
13. Heyes MP (1987) Hypothesis: a role for quinolinic acid in the neuropathology of glutaric aciduria type I. *Can J Neurol Sci* 14:441–443
14. Varadkar S, Surtees R (2004) Glutaric aciduria type I and kynurenine pathway metabolites: a modified hypothesis. *J Inher Metab Dis* 27:835–842
15. Pérez-De La Cruz V, Carrillo-Mora P, Santamaría A (2012) Quinolinic acid, an endogenous molecule combining excitotoxicity, oxidative stress and other toxic mechanisms. *Int J Tryptophan Res* 5:1–8
16. Ribeiro CAJ, Grando V, Dutra Filho CS, Wannmacher CM, Wajner M (2006) Evidence that quinolinic acid severely impairs energy metabolism through activation of NMDA receptors in striatum from developing rats. *J Neurochem* 99:1531–1542
17. Dalcin KB, Rosa RB, Schmidt AL, Winter JS, Leipnitz G, Dutra-Filho CS, Wannmacher CM, Porciúncula LO et al (2007) Age and brain structural related effects of glutaric and 3-hydroxyglutaric acids on glutamate binding to plasma membranes during rat brain development. *Cell Mol Neurobiol* 27:805–818
18. de Oliveira MF, Hagen ME, Pederzoli CD, Sgaravatti AM, Durigon K, Testa CG, Wannmacher CM, de Souza Wyse AT et al (2003) Glutaric acid induces oxidative stress in brain of young rats. *Brain Res* 964:153–158
19. Figuera MR, Royes LF, Furian AF, Oliveira MS, Fiorenza NG, Frussa-Filho R, Petry JC, Coelho RC et al (2006) GM1 ganglioside prevents seizures, Na⁺,K⁺-ATPase activity inhibition and oxidative stress induced by glutaric acid and pentylentetrazole. *Neurobiol Dis* 22:611–623
20. Jafari P, Braissant O, Bonafé L, Ballhausen D (2011) The unsolved puzzle of neuropathogenesis in glutaric aciduria type I. *Mol Genet Metab* 104:425–437
21. Kölker S, Ahlemeyer B, Krieglstein J, Hoffmann GF (1999) 3-Hydroxyglutaric and glutaric acids are neurotoxic through NMDA receptors in vitro. *J Inher Metab Dis* 22:259–262
22. Kölker S, Ahlemeyer B, Krieglstein J, Hoffmann GF (2001) Contribution of reactive oxygen species to 3-hydroxyglutarate neurotoxicity in primary neuronal cultures from chick embryo telencephalons. *Pediatr Res* 50:76–82
23. Kölker S, Ahlemeyer B, Hühne R, Mayatepek E, Krieglstein J, Hoffmann GF (2001) Potentiation of 3-hydroxyglutarate neurotoxicity following induction of astrocytic iNOS in neonatal rat hippocampal cultures. *Eur J Neurosci* 13:2115–2122
24. Kölker S, Okun JG, Ahlemeyer B, Wyse AT, Hörster F, Wajner M, Kohlmüller D, Mayatepek E et al (2002) Chronic treatment with glutaric acid induces partial tolerance to excitotoxicity in neuronal cultures from chick embryo telencephalons. *J Neurosci Res* 68:424–431
25. Kölker S, Köhr G, Ahlemeyer B, Okun JG, Pawlak V, Hörster F, Mayatepek E, Krieglstein J et al (2002) Ca²⁺ and Na⁺ dependence of 3-hydroxyglutarate-induced excitotoxicity in primary neuronal cultures from chick embryo telencephalons. *Pediatr Res* 52:199–206
26. Kölker S, Koeller DM, Sauer S, Hörster F, Schwab MA, Hoffmann GF, Ullrich K, Okun JG (2004) Excitotoxicity and bioenergetics in glutaryl-CoA dehydrogenase deficiency. *J Inher Metab Dis* 27:805–812
27. Kölker S, Sauer SW, Okun JG, Hoffmann GF, Koeller DM (2006) Lysine intake and neurotoxicity in glutaric aciduria type I: towards a rationale for therapy? *Brain* 129:e54
28. Latini A, Borba Rosa R, Scussiato K, Llesuy S, Belló-Klein A, Wajner M (2002) 3-Hydroxyglutaric acid induces oxidative stress and decreases the antioxidant defenses in cerebral cortex of young rats. *Brain Res* 956:367–373
29. Latini A, Scussiato K, Leipnitz G, Dutra-Filho CS, Wajner M (2005) Promotion of oxidative stress by 3-hydroxyglutaric acid in rat striatum. *J Inher Metab Dis* 28:57–67
30. Latini A, Ferreira GC, Scussiato K, Schuck PF, Solano AF, Dutra-Filho CS, Vargas CR, Wajner M (2007) Induction of oxidative stress by chronic and acute glutaric acid administration to rats. *Cell Mol Neurobiol* 27:423–438
31. Magni DV, Furian AF, Oliveira MS, Souza MA, Lunardi F, Ferreira J, Mello CF, Royes LF et al (2009) Kinetic characterization of I-[(3)H]glutamate uptake inhibition and increase oxidative damage induced by glutaric acid in striatal synaptosomes of rats. *Int J Dev Neurosci* 27:65–72
32. Olivera-Bravo S, Fernández A, Sarlabós MN, Rosillo JC, Casanova G, Jiménez M, Barbeito L (2011) Neonatal astrocyte damage is

- sufficient to trigger progressive striatal degeneration in a rat model of glutaric acidemia-I. *PLoS One* 6:e20831
33. Olivera S, Fernandez A, Latini A, Rosillo JC, Casanova G, Wajner M, Cassina P, Barbeito L (2008) Astrocytic proliferation and mitochondrial dysfunction induced by accumulated glutaric acidemia I (GAI) metabolites: possible implications for GAI pathogenesis. *Neurobiol Dis* 32:528–534
 34. Porciúncula LO, Dal-Pizzol A Jr, Coitinho AS, Emanuelli T, Souza DO, Wajner M (2000) Inhibition of synaptosomal [3H]glutamate uptake and [3H]glutamate binding to plasma membranes from brain of young rats by glutaric acid in vitro. *J Neurol Sci* 173:93–96
 35. Porciúncula LO, Emanuelli T, Tavares RG, Schwarzbold C, Frizzo ME, Souza DO, Wajner M (2004) Glutaric acid stimulates glutamate binding and astrocytic uptake and inhibits vesicular glutamate uptake in forebrain from young rats. *Neurochem Int* 45:1075–1086
 36. Rosa RB, Schwarzbold C, Dalcin KB, Ghisleni GC, Ribeiro CA, Moretto MB, Frizzo ME, Hoffmann GF et al (2004) Evidence that 3-hydroxyglutaric acid interacts with NMDA receptors in synaptic plasma membranes from cerebral cortex of young rats. *Neurochem Int* 45:1087–1094
 37. Rosa RB, Dalcin KB, Schmidt AL, Gerhardt D, Ribeiro CA, Ferreira GC, Schuck PF, Wyse AT et al (2007) Evidence that glutaric acid reduces glutamate uptake by cerebral cortex of infant rats. *Life Sci* 81:1668–1676
 38. Stokke O, Goodman SI, Moe PG (1976) Inhibition of brain glutamate decarboxylase by glutarate, glutaconate, and beta-hydroxyglutarate: explanation of the symptoms in glutaric aciduria? *Clin Chim Acta* 66:411–415
 39. Wajner M, Kölker S, Souza DO, Hoffmann GF, de Mello CF (2004) Modulation of glutamatergic and GABAergic neurotransmission in glutaryl-CoA dehydrogenase deficiency. *J Inher Metab Dis* 27:825–828
 40. Colín-González AL, Paz-Loyola AL, Serratos I, Seminotti B, Ribeiro CA, Leipnitz G, Souza DO, Wajner M et al (2015) Toxic synergism between quinolinic acid and organic acids accumulating in glutaric acidemia type I and in disorders of propionate metabolism in rat brain synaptosomes: relevance for metabolic acidemias. *Neuroscience* 308:64–74
 41. Seminotti B, Amaral AU, Ribeiro RT, Rodrigues MD, Colín-González AL, Leipnitz G, Santamaría A, Wajner M (2016) Oxidative stress, disrupted energy metabolism, and altered signaling pathways in glutaryl-CoA dehydrogenase knockout mice: potential implications of quinolinic acid toxicity in the neuropathology of glutaric acidemia type I. *Mol Neurobiol* 53:6459–6475
 42. Pierozan P, Biasibetti H, Schmitz F, Ávila H, Parisi MM, Barbeituana F, Wyse AT, Pessoa-Pureur R (2016) Quinolinic acid neurotoxicity: differential roles of astrocytes and microglia via FGF-2-mediated signaling in redox-linked cytoskeletal changes. *Biochim Biophys Acta* 1863:3001–3014
 43. Ferreira GC, Tonin A, Schuck PF, Viegas CM, Ceoloto PC, Latini A, Perry ML, Wyse AT et al (2007) Evidence for a synergistic action of glutaric and 3-hydroxyglutaric acids disturbing rat brain energy metabolism. *Int J Dev Neurosci* 25:391–398
 44. Pierozan P, Ferreira F, de Lima BO, Pessoa-Pureur R (2015) Quinolinic acid induces disrupts cytoskeletal homeostasis in striatal neurons. Protective role of astrocyte-neuron interaction. *J Neurosci Res* 93:268–284
 45. Hu X, Zhang D, Pang H, Caudle WM, Li Y, Gao H, Liu Y, Qian L et al (2008) Macrophage antigen complex-1 mediates reactive microgliosis and progressive dopaminergic neurodegeneration in the MPTP model of Parkinson's disease. *J Immunol* 181:7194–7204
 46. LeBel CP, Ali SF, McKee M, Bondy SC (1990) Organometal-induced increases in oxygen reactive species: the potential of 2', 7'-dichlorofluorescein diacetate as an index of neurotoxic damage. *Toxicol Appl Pharmacol* 104:17–24
 47. Aksenov MY, Markesbery WR (2001) Changes in thiol content and expression of glutathione redox system genes in the hippocampus and cerebellum in Alzheimer's disease. *Neurosci Lett* 302:141–145
 48. Browne RW, Armstrong D (1998) Reduced glutathione and glutathione disulfide. *Methods Mol Biol* 108:347–352
 49. Maiuri MC, Zalckvar E, Kimchi A, Kroemer G (2007) Self-eating and self-killing: crosstalk between autophagy and apoptosis. *Nat Rev Mol Cell Biol* 8:741–752
 50. Ankarcróna M, Dypbukt JM, Bonfoco E, Zhivotovskiy B, Orrenius S, Lipton SA, Nicotera P (1995) Glutamate-induced neuronal death: a succession of necrosis or apoptosis depending on mitochondrial function. *Neuron* 15:961–973
 51. Peng TI, Jou MJ (2010) Oxidative stress caused by mitochondrial calcium overload. *Ann N Y Acad Sci* 1201:183–188
 52. Gutteridge JM, Halliwell B (2000) Free radicals and antioxidants in the year 2000. A historical look to the future. *Ann N Y Acad Sci* 899:136–147
 53. Circu ML, Aw TY (2012) Glutathione and modulation of cell apoptosis. *Biochim Biophys Acta* 1823:1767–1777
 54. Hardeland R (2009) Neuroprotection by radical avoidance: search for suitable agents. *Molecules* 14:5054–5102
 55. Hardeland R, Coto-Montes A, Poeggeler B (2003) Circadian rhythms, oxidative stress, and antioxidative defense mechanisms. *Chronobiol Int* 20:921–962
 56. Andrabi SA, Sayeed I, Siemen D, Wolf G, Hom TF (2004) Direct inhibition of the mitochondrial permeability transition pore: a possible mechanism responsible for anti-apoptotic effects of melatonin. *FASEB J* 18:869–871
 57. Entrena A, Camacho ME, Carrión MD, López-Cara LC, Velasco G, León J, Escames G, Acuña-Castroviejo D et al (2005) Kynurenamines as neural nitric oxide synthase inhibitors. *J Med Chem* 48:8174–8181
 58. Sainz RM, Mayo JC, Rodriguez C, Tan DX, Lopez-Burillo S, Reiter RJ (2003) Melatonin and cell death: differential actions on apoptosis in normal and cancer cells. *Cell Mol Life Sci* 60:1407–1426
 59. Pandi-Perumal SR, Srinivasan V, Maestroni GJ, Cardinali DP, Poeggeler B, Hardeland R (2006) Melatonin: nature's most versatile biological signal? *FEBS J* 273:2813–2838
 60. Acuña-Castroviejo D, Escames G, Rodriguez MI, Lopez LC (2007) Melatonin role in the mitochondrial function. *Front Biosci* 12:947–963
 61. Wang X (2009) The antiapoptotic activity of melatonin in neurodegenerative diseases. *CNS Neurosci Ther* 15:345–357
 62. Pierozan P, Zamoner A, Soska ÁK, de Lima BO, Reis KP, Zamboni F, Wajner M, Pessoa-Pureur R (2012) Signaling mechanisms downstream of quinolinic acid targeting the cytoskeleton of rat striatal neurons and astrocytes. *Exp Neurol* 233:391–399
 63. Stípek S, Stastný F, Pláteník J, Crkavská J, Zima T (1997) The effect of quinolinate on rat brain lipid peroxidation is dependent on iron. *Neurochem Int* 30:233–237
 64. von Bernhardt R, Eugenín-von Bernhardt L, Eugenín J (2015) Microglial cell dysregulation in brain aging and neurodegeneration. *Front Aging Neurosci* 7:124
 65. Syed Mortadza SA, Wang L, Li D, Jiang LH (2015) TRPM2 channel-mediated ROS-sensitive Ca²⁺ signaling mechanisms in immune cells. *Front Immunol* 6:407